Molecular Therapy
Methods & Clinical Development
Original Article

Gesicles packaging dCas9-VPR ribonucleoprotein complexes can combine with vorinostat and promote HIV proviral transcription

Michaela A. Fisher,[1] Waj Chaudhry,[1] and Lee A. Campbell[1]

[1]Laboratory of Preclinical Neurobiology, Department of Neuroscience, Washington, DC, USA

Despite the success of combination antiretroviral therapy (cART) in HIV treatment, a cure for HIV remains elusive. Scientists postulate that HIV latent reservoirs may be a vital target in curative strategies. Vorinostat is a latency-reversing agent that has demonstrated some effectiveness in reactivating latent HIV, but complementary therapies may be essential to enhance its efficacy. One such approach may utilize the CRISPR-Cas9 system, which has evolved to include transcriptional activators such as dCas9-VPR. In this study, we explored the effects of combining vorinostat coupled with gesicle-mediated delivery of dCas9-VPR in promoting the transcription of integrated HIV proviruses in HIV-NanoLuc CHME-5 microglia and J-Lat 10.6 lymphocytes. We confirmed that dCas9-VPR ribonucleoprotein complexes can be packaged into gesicles and application to cells successfully induced HIV transcription through interactions with the HIV LTR. Vorinostat also induced significant increases in proviral transcription but generated inhibition of cellular proliferation (microglia) or cell viability (lymphocytes) starting at 1,000 nM and higher concentrations. Experiments combining dCas9-VPR gesicles and vorinostat confirmed the enhanced transcriptional activation of the HIV provirus in microglia but not lymphocytes. Thus, a combination of dCas9-VPR gesicles with other latency-reversing agents may provide a complementary method to activate latent HIV in future studies utilizing patient-derived cells or small animal models.

INTRODUCTION

The human immunodeficiency virus (HIV) is a global health epidemic that since its inception, has infected 85.6 million individuals and resulted in a loss of 40.4 million lives.[1] HIV is a lentivirus that functions by attacking the body's immune system, primarily targeting CD4+ T cells. The replication cycle within CD4+ T cells is cytotoxic, resulting in their destruction and a steady decline in their overall population within the body.[2,3] If left untreated, this infection can progress to the acquired immunodeficiency syndrome, characterized either by CD4+ cell count falling below 200 cells/mm^3 or the development of more opportunistic infections regardless of CD4+ cell count. The current standard of care is combination antiretroviral therapy (cART), which effectively suppresses viral replication, delays disease progression, decreases viral loads to undetectable levels, and prevents transmission to uninfected individuals.[4,5] However, despite the success of cART, a cure for HIV remains elusive.

It is postulated that HIV latent reservoirs, in which cells and tissues remain in a reversible state of non-productive infection,[6–8] may be a vital target in curative strategies. These viral reservoirs are impervious to cART, and due to their resting phenotype, evade recognition by the immune system.[4,9] Furthermore, treatment interruption results in reservoir activation, igniting viral rebound within weeks.[10,11] The latent HIV reservoir exists in a variety of cells and tissues throughout the body including CD4+ T cells, mononuclear macrophages, dendritic cells, hemopoietic progenitor cells, astrocytes, and microglia.[12–18]

One therapeutic strategy, referred to as the "shock and kill" method, has been extensively studied in an aim to find a cure for HIV. This strategy utilizes various latency-reversing agents to induce viral expression in latently infected cells, resulting in recognition and elimination by the immune system or antiretroviral therapies.[19,20] Among the latency-reversing agents, vorinostat is a potent histone deacetylase (HDAC) inhibitor that has been found to effectively reactivate latent HIV.[21–23] However, clinical trials using vorinostat have shown modest efficacy in its ability to activate latent HIV and subsequently decrease the number of latently infected cells.[19,24] Thus, alternative and/or complementary strategies may need to be utilized to enhance its effectiveness.

In addition to pharmacological approaches, the CRISPR-Cas9 gene editing system is an alternative method that is being explored for HIV therapies. Various compositions of this system have been utilized to either trigger HIV inactivation or induce HIV transcription. The CRISPR-Cas9 system is generally composed of the Cas9 endonuclease and a guide RNA (gRNA) sequence that is next to a protospacer adjacent motif site (typically -NGG). In a sequence-specific

Received 29 June 2023; accepted 29 January 2024;
https://doi.org/10.1016/j.omtm.2024.101203.

Correspondence: Lee Campbell, PhD, Georgetown University Medical Center, Department of Neuroscience, EG07 New Research Building, 3970 Reservoir Rd, NW, Washington, DC 20057, USA.
E-mail: lac89@georgetown.edu

manner, this system causes cleavage of double-stranded DNA, which is followed by random based pair insertions or deletions (indels) due to DNA repair, and ultimately results in an introduction of permanent mutations within the DNA sequence.[25,26] Investigators have successfully utilized this system *in vitro* and *in vivo* to both mutate key regions in the HIV provirus that are required for replication (e.g., long terminal repeat, Gag-Pol, gp120, and others) or perform complete proviral excision.[27,28] Moreover, clinical trials utilizing CRISPR-Cas9 for HIV eradication are now under way (ClinicalTrials.gov identifiers: NCT05144386, NCT05143307). Alternatively, the gene editing system can be used as an activator when composed of an endonuclease dead version of Cas9 (dCas9) fused to a transcription activation domain. In combination with a gRNA, these proteins can target the HIV promoter region, the long terminal repeat (LTR), and activate viral transcription.[27,29,30] Several systems utilizing various transcription factors including VP16 (from herpes virus, targets Gal4-binding sites), VP64 (four tandem copies of VP16), p65 (part of the NF-κB transcriptional complex), Rta (from Epstein-Barr virus, can bind to Rta responsive element or act through protein recruitment), and p300 (histone acetyltransferase) have been shown to effectively cause HIV activation.[29,31–34] Of these, a hybrid VP64-p65-Rta tripartite activator, referred to as VPR, has been found to have robust effects in increasing transcriptional activation.[33,35,36]

A majority of CRISPR-Cas9 systems currently utilize viral vectors, including adeno-associated viruses and lentiviruses, to express Cas9 and gRNA sequences in eukaryotic cells. In comparison, our lab has previously utilized a microvesicle called a gesicle[37] to package Cas9 and its associated gRNA as a ribonucleoprotein (RNP) complex. Gesicles are produced by an overexpression of vesicular stomatitis virus G glycoprotein (VSV-G) and allow for rapid delivery, but transient expression of Cas9 RNP, with the goal of reducing potential off-target effects. We have previously utilized this method to mutate or excise integrated HIV proviruses by delivering Cas9 targeted to the HIV LTR. However, it has not been established if utilizing gesicles to package the dCas9-VPR variant can effectively induce HIV transcriptional activation.

In this study, we characterized whether dCas9-VPR could be packaged into gesicles and if gesicle treatment would affect the proviral transcription of HIV-NanoLuc CHME-5 microglia and J-Lat 10.6 lymphocytes. Furthermore, we explored the synergistic effects of vorinostat coupled with gesicle-mediated delivery of dCas9-VPR on promoting HIV transcription. We found that dCas9-VPR gesicles can induce HIV transcription alone, or in combination with vorinostat by acting on the HIV LTR. Thus, gesicles packaging dCas9-VPR may be an attractive alternative approach to enhance proviral transcription alone or in combination with other latency-reversing agents.

RESULTS

dCas9-VPR can be packaged into gesicles and promote HIV proviral transcription

Our first goal was to confirm that dCas9-VPR ribonucleoprotein complexes could be packaged into gesicles. Gesicles are produced in HEK293FT cells via a calcium phosphate transfection that utilizes a gesicle packaging mix containing CherryPicker Red, VSV-G, a specific Cas9 variant, and a gRNA directed to the NF-κB II binding site on the HIV LTR (Figure 1A). Three specific variants of Cas9: Cas9, Cas9-VPR, or dCas9-VPR were utilized to compare their effects on HIV transcription and site-specific mutation (Figure 1B). Cas9 is a bacterial endonuclease that couples with the gRNA to cleave DNA via complementary base pairing.[38,39] Dead Cas9 (dCas9) lacks its endonuclease activity, allowing for CRISPR-mediated gene silencing.[40] Cas9-VPR and dCas9-VPR are fusion proteins in which either Cas9 or dCas9 fuse with VP64-p65-Rta (VPR), a tripartite activator.[35] We anticipated that only dCas9-VPR gesicles would promote HIV transcription and would be free of site-specific mutations.

After transfection, gesicles were collected and purified by ultracentrifugation from the concentrated media of HEK293FT producer cells. Western blot analysis was performed on both the cell lysate and collected gesicles to examine the expression of VSV-G, Cas9 variants, and actin. Untreated producer cells and media were used as controls. Western blot analysis of lysates (L) and gesicles (G) from transfected cells revealed the presence of VSV-G and Cas9 variants (Figure 1C, left and middle blots). Neither control lysates nor media expressed VSV-G or Cas9. Next, the controls, lysates, and gesicles were all analyzed for expression of actin. Western blot analysis detected actin within each of the lysates but with minimal expression in the gesicles or media control (Figure 1C right blot). Additionally, because gesicles were produced in the absence of a packaging facilitator such as the i-Dimerize system, these data suggest that dCas9-VPR can be stochastically packaged into gesicles.

We next applied gesicles carrying their respective Cas9 variants to HIV-NanoLuc CHME-5 microglia, which contain integrated HIV proviruses that express NanoLuciferase under control of the HIV LTR.[41] Gesicles were allowed to enter the cells over a course of 16 h, and live cell imaging showed the uptake of CherryPicker Red fluorescent gesicles over time (Figure 1D). After the time course, a luciferase assay was performed that showed a 2-fold increase of HIV transcriptional activity in cells specifically treated with dCas9-VPR gesicles.

dCas9-VPR gesicles do not cause mutation or excision of the HIV provirus

We next performed a PCR assay to determine if excision or mutation occurred by dCas9-VPR gesicle treatment. A full-length integrant of the HIV provirus is located at the ROSA26 locus. Thus, we amplified a 1,015-base pair (bp) region that spans through this locus into the NanoLuciferase region of the provirus, effectively encompassing the entire 5′LTR (Figure 2A). We also prepared a primer set to amplify ∼500 bp of glyceraldehyde 3-phosphate dehydrogenase (GAPDH) as a control.

Because the HIV provirus contains two identical LTR regions (5′ and 3′ end), complete proviral excision can occur. In this situation, the internal primer binding site would be missing, leading to a loss of PCR

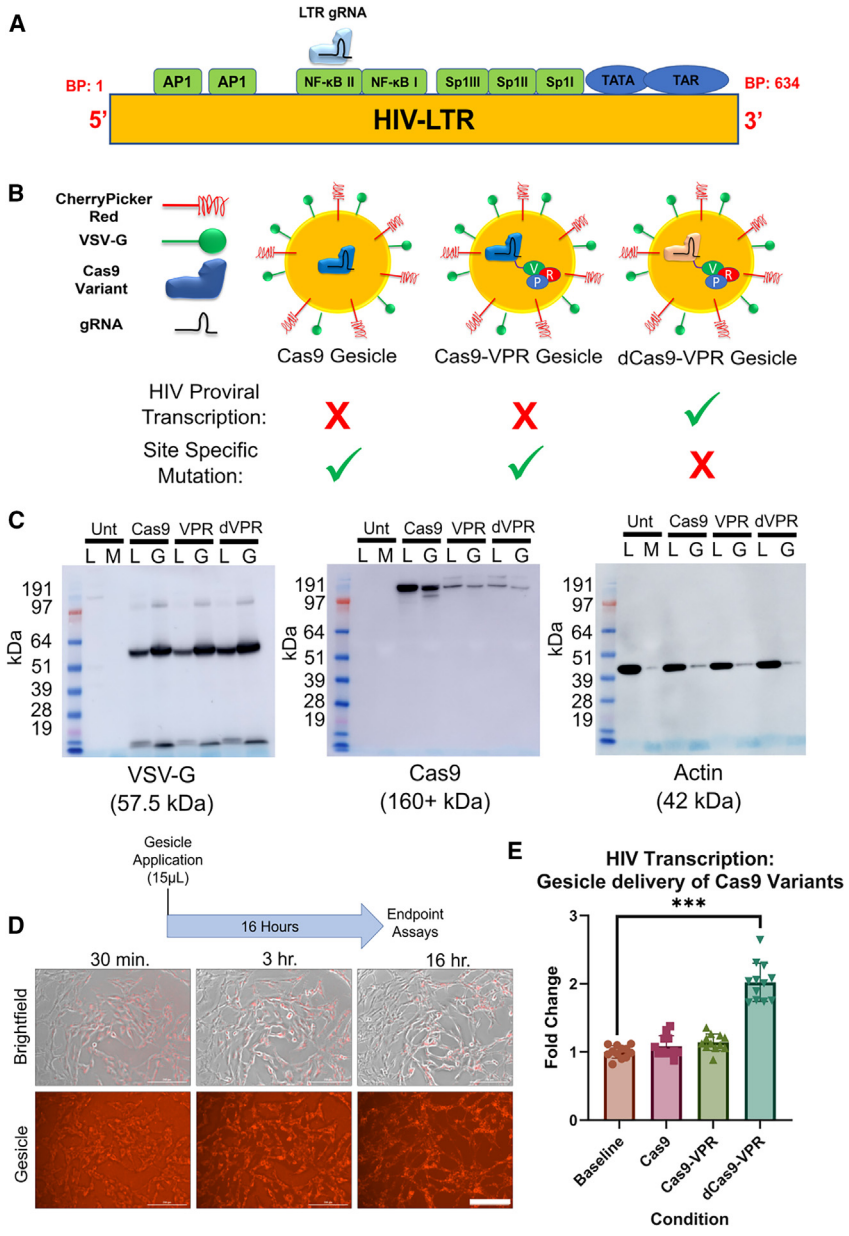

Figure 1. dCas9-VPR gesicles increase HIV proviral transcription

Gesicles were prepared with three Cas9 variants to determine if gesicle-mediated delivery of dCas9-VPR would promote HIV proviral transcription. (A) A single gRNA sequence targeted to the NF-κB II binding site of the long terminal repeat was used in conjunction with Cas9 variants. (B) Schematic of gesicles packaging Cas9 variants with expected results from gesicle treatment. (C) Western blot analysis identifies protein expression and confirms successful packaging of Cas9 variants into gesicles. Samples from untreated HEK293FT cells (unt) were used as a negative control. Cell lysates (L), conditioned media (M), and gesicles (G) were assayed. VSV-G (57.5 kDa) was expressed in both gesicles and lysates of cells transfected with the gesicle packaging mix, but not in untreated cells. Cas9 variants (~160+ kDa) were expressed in both gesicles and lysates of transfected cells, but not in untreated cells. Actin (42 kDa) was highly expressed in the cell lysates, but minimally present in media or gesicles. (D) Prepared gesicles were used to treat HIV-NanoLuc CHME-5 microglia for a total of 16 h. Time course images of gesicle application and entry are provided in the panel. Scale bar, 200 μm. (E) Luciferase assay for proviral activity after gesicle treatment of Cas9 variants. n = 12 (six separate gesicle preparations, two technical replicates per gesicle preparation). Statistical analysis was performed by an ordinary one-way ANOVA with Dunnett's multiple comparisons test vs. baseline luminescence. ***$p < 0.001$. Data are expressed as the mean (SD).

product. We performed PCR on the genomic DNA purified from gesicle-treated cells and observed a decrease in the 1,015-bp amplicon in those receiving Cas9 (Figure 2B). Densitometric analysis against GAPDH confirmed a significant decrease in band density of Cas9-treated cells, but not those treated with dCas9-VPR. The resulting 1,015-bp amplicons were then excised, gel purified, and run through Sanger sequencing to ultimately perform tracking of indels by decomposition (TIDE) analysis[42] (Figure 2C). This method allows for the identification and quantification of site-specific mutations. Our analysis revealed that Cas9-treated cells showed significant mutation efficiency (~2.4%) when compared with cells exposed to dCas9-VPR (~0.7%), where 2% is the limit of detection for site-specific mutations.

Taken together, delivery of dCas9-VPR by gesicles results in a significant increase in proviral transcription but does not cause excision or mutation of the HIV provirus.

Vorinostat increases HIV proviral transcription but inhibits cellular proliferation

Vorinostat (VOR) is a histone deacetylase (HDAC) inhibitor that can induce alterations in transcription.[43] To examine the effects of VOR on HIV proviral transcription, HIV-NanoLuc CHME-5 microglia were treated with VOR, as well as lipopolysaccharide (LPS) and Resiquimod (R848). LPS is a toll-like receptor (TLR) agonist that acts on TLR4,[44] and R848 is also a toll-like receptor agonist but acts by binding to TLR7 and TLR8. Activation of both these receptors is correlated with elevated levels of NF-κB-mediated transcription, which is known to enhance HIV proviral activity.

We first treated cells with various concentrations of LPS, R848, and VOR ranging from 0.1 to 100,000 nM. After a 16-h incubation period, a luciferase assay was used to examine the effects of LPS, R848, and VOR on HIV proviral transcription. As expected, LPS increased proviral transcription at each concentration, with a peak at 10,000 ng/mL (4-fold increase) (Figure 3A). R848 also caused significant increases in

Table 1. List of primer sets used

Primer description	Sequence 5′ to 3′
ROSA26 FWD- for HIV-NanoLuc CHME-5 LTR amplification	5′-CTCTGCTGCCTCCTGTCTTCTG-3′
NLuc REV- for HIV-NanoLuc CHME-5 LTR amplification	5′-CGGACACCCCGAGATTCTGAAAC-3′
LTR REV- nested primer for TIDE analysis	5′-AGTCACACAACAGACGGGCAC-3′
GAPDH FWD- for GAPDH amplification	5′-ACCACAGTCCATGCCATCACTGCCAC-3′
GAPDH REV- for GAPDH amplification	5′-AGGTCCACCACCCTGTTGCTGTAGCC-3′
JLat10.6 FWD- for J-Lat 10.6 LTR amplification	5′-ATAGTAATCGCTCTGACTGCTCCATC-3′
JLat10.6 REV- for J-Lat 10.6 LTR amplification	5′ CCGCTTAATACTGACGCTCTCGC-3′

transcription. However, significance was only observed starting at a 100-nM concentration (2-fold increase) (Figure 3B). In comparison, treatment with VOR resulted in large, however non-dose-dependent increases in proviral transcription. Significant increases in transcription were observed at 100 nM (2-fold increase), 1,000 nM (∼12-fold increase), 10,000 nM (∼8-fold increase), and 100,000 nM (∼6-fold increase) (Figure 3C). Thus, proviral transcription occurred to the greatest extent when cells were treated with VOR at a concentration of 1,000 nM but decreased at higher concentrations.

Taking this into consideration, we wanted to evaluate the effect of VOR treatment on cell viability and proliferation. HIV-NanoLuc CHME-5 microglia were treated then analyzed after 16 h using a luminescence-based ATP assay for viability. Treatment of the cells with VOR did not result in any significant changes in cell viability (Figure 3D). Because VOR is known to have anti-proliferative properties, we used Hoechst staining to count cells post treatment. We found that VOR concentrations of 1,000-100,000 nM caused a significant decrease in cellular proliferation (Figure 3E). Due to these results, our subsequent combination experiments utilized VOR at 100 nM, which activated proviral transcription but did not result in decreased proliferation, and at 1,000 nM, which had the highest proviral activation, but significantly decreased proliferation.

dCas9-VPR gesicles can combine with vorinostat and enhance HIV proviral transcription

We performed combination experiments by pre-treating HIV-NanoLuc CHME-5 microglia with VOR for 1 h, followed by gesicle application directly into the media containing VOR. Live cell imaging confirmed the uptake of gesicles in the presence of VOR at both concentrations (Figure 4A). Subsequent luciferase assays after the 16-h time course revealed that dCas9-VPR enhanced proviral transcription when combined with 100 nM and 1,000 nM VOR (Figure 4B). Interestingly, the other variants—Cas9 and Cas9-VPR—showed a significant decrease in proviral transcription when combined with VOR at 1,000 nM (Figure 4B).

We also analyzed excision and mutation of the HIV provirus as previously described. Results confirmed that dCas9-VPR gesicles do not cause significant excision or mutation even when combined with VOR at either concentration. However, the excision assay showed a decrease in the 1,015-bp amplicon with Cas9 under both 100 nM and 1,000 nM VOR (Figure 5A), which was significant after densitometric analysis (Figure 5B). Interestingly, TIDE analysis showed greater mutation efficiency when combining Cas9 with VOR at both 100 nM and 1,000 nM (Figure 5C and 5D). Together, the data suggest that dCas9-VPR gesicles can combine with VOR in HIV-NanoLuc CHME-5 microglia to enhance proviral transcription without causing site-specific mutation or proviral excision.

dCas9-VPR gesicles reactivate latent provirus in J-Lat 10.6 lymphocytes

We next tested the efficacy of dCas9-VPR gesicles to activate a latent HIV provirus in J-Lat 10.6 lymphocytes.[45,46] This model contains a single integrant of a modified provirus that expresses enhanced green fluorescent protein (EGFP) upon reactivation. We first established a dose-response against vorinostat utilizing the same concentrations as previously described (0–100,000 nM). Live cell imaging confirmed latency reversal using vorinostat (Figure 6A). We then utilized western blot analysis using an antibody specific to EGFP to quantify latency reversal, where we observed a significant increase in EGFP expression at concentrations of 1,000 nM and above (Figure 6B). Interestingly, as shown in our western blots, a decrease in actin immunoreactivity correlated with increased EGFP expression. Because of this, we assayed cell viability through trypan blue staining and showed a significant decrease in cell viability starting at a concentration of 1,000 nM (Figure 6C). Our next experiments focused specifically on Cas9 and dCas9-VPR gesicles to determine alterations in proviral latency. When comparing the LTR targeted gRNA sequences of HIV-NanoLuc CHME-5 and J-Lat 10.6 lymphocytes, there is a single base pair difference at the second nucleotide (G vs. C, see materials and methods). Thus, we first performed molecular-based TIDE analysis and confirmed that the J-Lat 10.6 specific gRNA was interacting in the correct area (Figure 7A), where results showed significant site-specific mutations using Cas9 gesicles but not dCas9-VPR gesicles as expected. Further application of Cas9 or dCas9-VPR gesicles were used to assay latency reversal through EGFP expression either alone or in combination with 1,000 nM vorinostat (the first concentration that resulted in significant EGFP expression). Combination experiments were performed as previously described, with a 1-h pretreatment of vorinostat prior to gesicle addition. Cells were exposed to vorinostat and gesicles concurrently for the rest of the treatment time course. Our observations of live cell imaging showed that dCas9-VPR gesicles (and Cas9 gesicles) induce cellular clumping, but only dCas9-VPR gesicles caused EGFP expression (Figure 7B). Western blot analysis revealed that dCas9-VPR gesicles significantly increased EGFP expression alone (Figures 7C and 7D) but not in combination with vorinostat (Figures 7C and 7D). In addition, we continued to observe alterations in actin expression after vorinostat treatment. Interestingly, latency reversal through dCas9-VPR gesicles did not seem to affect actin (Figure 7C). Therefore, we performed a viability

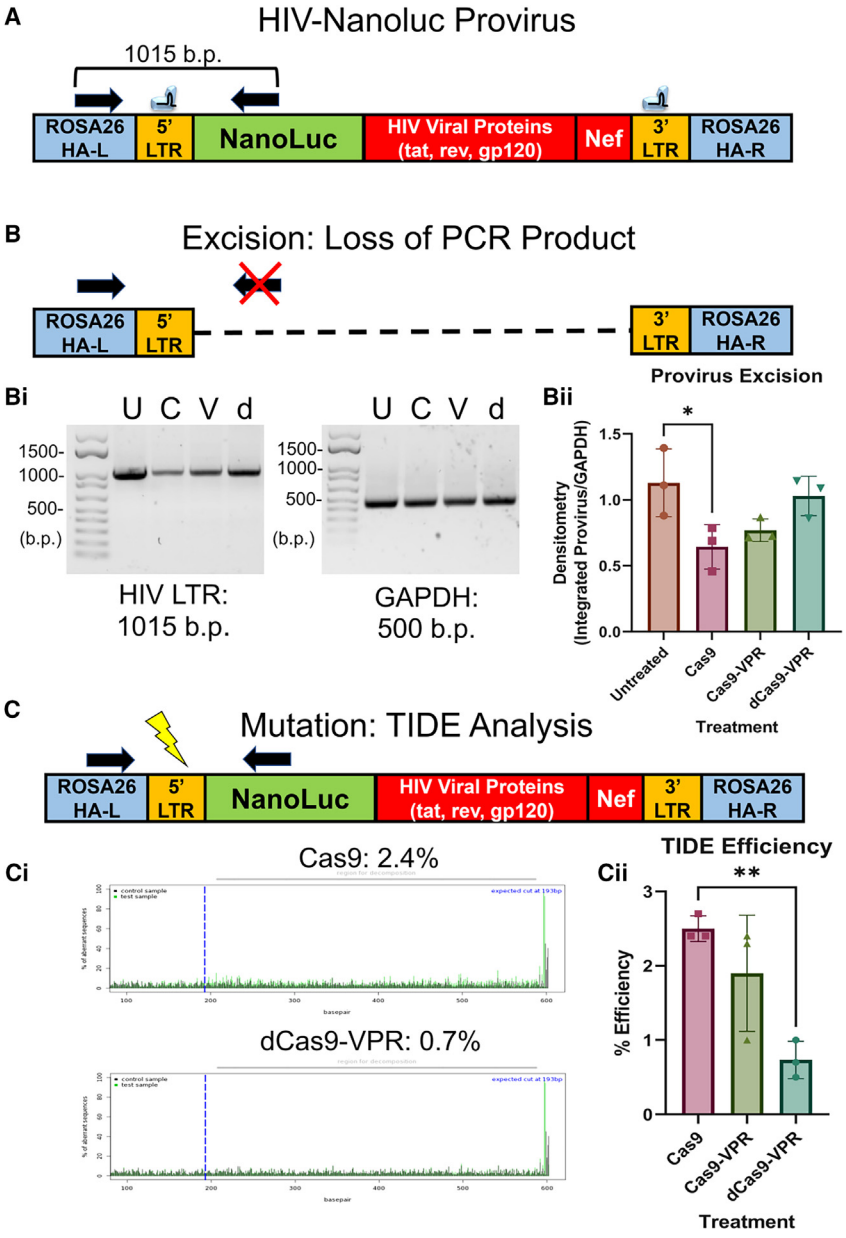

Figure 2. dCas9 gesicles do not results in excision or mutation of the HIV provirus

Two assays were performed to determine site-specific effects of Cas9 variants on the HIV provirus. (A) Schematic of the full-length HIV-NanoLuc provirus with PCR primer sets amplifying a 1,015-bp region spanning the HIV LTR. (B) Excision assay schematic. (Bi) Gel electrophoresis for the HIV LTR and GAPDH (U: untreated, C: Cas9, V: Cas9-VPR, d: dCas9-VPR). (Bii) Densitometric analysis of excision. n = 3 (three separate gesicle preparations). Statistical analysis was performed by an ordinary one-way ANOVA with Dunnett's multiple comparisons test vs. the untreated condition. *p = 0.0244. (C) TIDE analysis schematic. (Ci) TIDE Aberrant signal sequence graph. A rise in green bars denotes differences in untreated vs. experimental sample. (Cii) Efficiency score. n = 3 (three separate gesicle preparations). Statistical analysis was performed by an ordinary one-way ANOVA with Tukey's multiple comparisons test. **p = 0.01. Data are expressed as the mean (SD).

assay using trypan blue and found that gesicle treatment did not affect cell viability alone or in combination with vorinostat (Figure 7E). Together, these results confirm that gesicles can deliver dCas9-VPR to reactivate latently infected J-Lat 10.6 lymphocytes. However, further combination experiments utilizing vorinostat and other latency-reversing agents may be needed to optimize the effect.

DISCUSSION

Within this paper we demonstrate an alternative approach for latency reversal, utilizing gesicle-mediated delivery of dCas9-VPR. We characterized that dCas9-VPR can be packaged into gesicles and act on the HIV LTR to promote HIV proviral transcription. Furthermore, we demonstrate the synergistic capabilities of dCas9-VPR coupled with vorinostat on HIV proviral transcription.

Vorinostat is an HDAC inhibitor that has been extensively explored for its abilities to promote HIV transcription and reverse HIV latency.[21–23] In this study, we found that vorinostat was able to promote HIV transcription but also caused an inhibition of cellular proliferation in HIV-NanoLuc CHME-5 microglia. This is consistent with other studies that have identified that vorinostat inhibits cellular proliferation within various cell types.[47,48] Inhibition of cellular proliferation is common among HDAC inhibitors, including vorinostat, which is currently used for cancer treatment as it promotes antitumor activity.[49,50] While vorinostat has been found to effectively reactivate latent HIV, clinical trials have shown modest efficacy in its ability to activate latent HIV and subsequently, decrease the number of latently infected cells.[19,24] It is postulated that this can be due to several factors, including the viral reservoir being larger than originally thought, the inability to produce enough viral proteins to result in cell death, or because of an inadequate cytotoxic T lymphocyte response. Therefore, HDAC inhibitors alone may not be capable of reversing the entire latent reservoir.[51,52]

In addition to vorinostat, various forms of the CRISPR-Cas9 gene editing system have been recognized in their ability to modulate HIV proviral transcription.[29,30,33] When coupled with gRNAs, gene-specific transcriptional activation has been achieved using dCas9 fused to various transcription factors including the synergistic activation

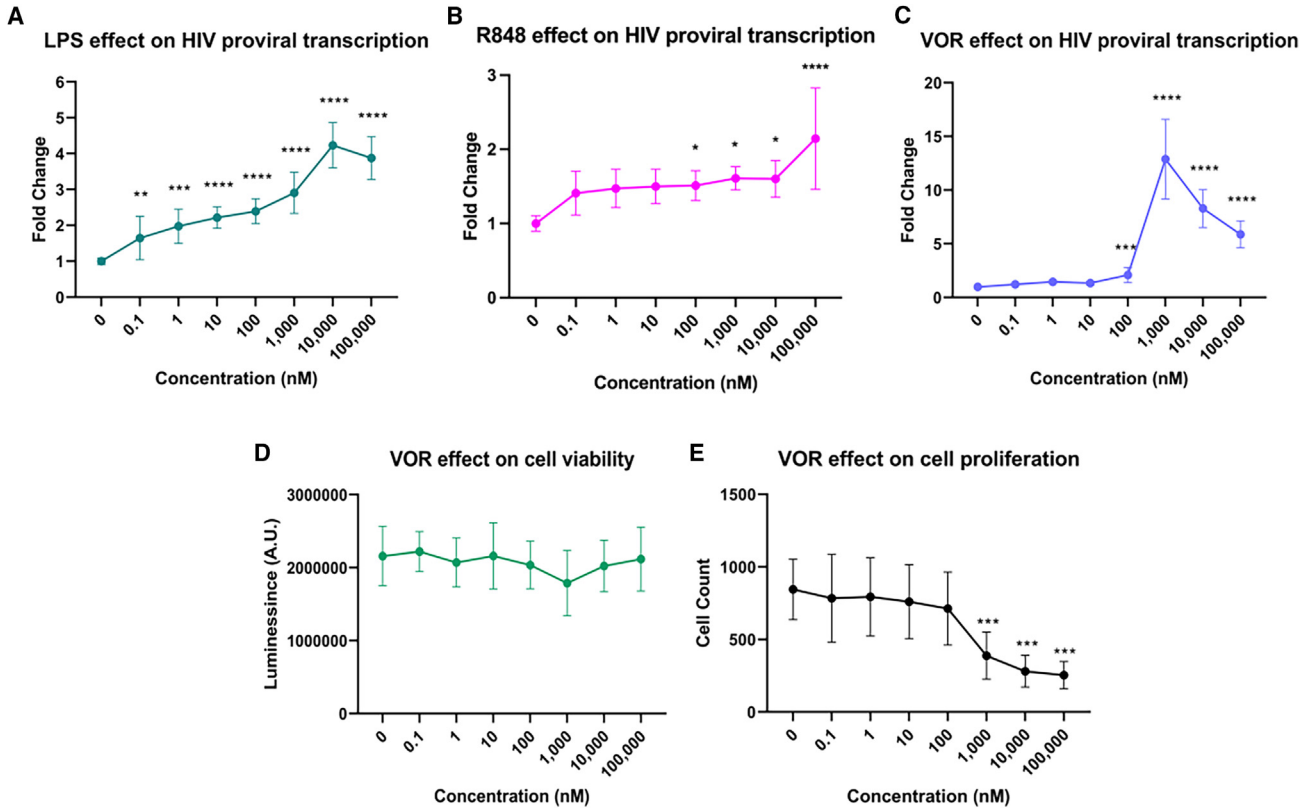

Figure 3. Effect of vorinostat on HIV proviral transcription in HIV-NanoLuc CHME-5 microglia

HIV-NanoLuc CHME-5 microglia were treated with LPS, R848, or VOR at increasing concentrations to create a dose-response relationship. Cells were incubated for 16 h and then examined via a luciferase assay. For the following experiments, statistical analysis was performed by an ordinary one-way ANOVA with Dunnett's multiple comparisons test vs. the untreated (0) control. (A) LPS dose-response curve. n = 6 (three cell passages, two technical replicates per passage). **p = 0.0077, ***p < 0.001, ****p < 0.0001. (B) R848 dose-response curve. n = 6 (three cell passages, two technical replicates per passage). *p = 0.0449, ****p < 0.0001. (C) VOR dose-response curve. n = 6 (three cell passages, two technical replicates per passage). ***p < 0.001, ****p < 0.0001. (D) ATP assay for cell viability. n = 6 (three cell passages, duplicate wells per passage). (E) Proliferation assay by cell counting of Hoechst-positive cells. n = 6 (three cell passages, two technical replicates per passage). ***p < 0.001. Data are expressed as the mean (SD).

mediator (SAM), VP16, VP64, p65, Rta, and p300.[29,31–33,53] Consistent with other studies, we found that dCas9-VPR can promote HIV proviral transcription, but in addition we explored a unique method for delivery of dCas9 and gRNA. Routinely, delivery of dCas9 and gRNA is achieved via plasmid transfection or viral transduction (via adeno-associated virus or lentivirus), both of which can induce transient or stable expression of Cas9 and/or gRNA. While effective, evidence suggests that sustained expression of these components can lead to off-target mutation events.[54–56] Another strategy allows for transient expression of CRISPR-Cas9 activity by delivery of a Cas9 RNP complex, commonly accomplished by electroporation or encapsulating the complex with cationic lipids.[57,58] Alternatively, delivery of the Cas9 RNP complex may occur via extracellular vesicles that are characterized as microvesicles, exosomes, or apoptotic bodies.[59] Within this study, we explored the ability of a microvesicle called a "gesicle" to package the Cas9 RNP complex. We confirmed that dCas9-VPR can be packaged as an RNP into gesicles and deliver its cargo to recipient cells within 16 h, leading to a significant increase in HIV proviral transcription.

To enhance the latency-reversing efficiency of vorinostat, we coupled vorinostat treatment with gesicle-mediated delivery of dCas9-VPR. Various studies have previously explored the synergistic abilities of vorinostat coupled with other latency-reversing agents.[60–62] For example, one study found that combined treatment with a PKA activator and HDAC inhibitor (vorinostat or trichostatin A) resulted in synergistic HIV-1 reactivation in latently infected cells.[61] Another study demonstrated that lentiviral transfection of SAM coupled with vorinostat treatment resulted in synergistic increases in latency reversal in J-Lat 9.2 and J-Lat 10.6 cell lines.[62] While additional studies have identified synergistic increases in latency reversal by coupling vorinostat with CRISPR activators, in this study we utilized gesicle-mediated delivery dCas9-VPR. This delivery method removes the process of transcription and translation associated with plasmid/virus methods of delivery, thus allowing for tighter temporal control of transcriptional activation. This unique characteristic may be beneficial when combining methodologies for latency reversal. For instance, vorinostat has a half-life of ~2 h.[63,64] Our data confirm that a 1-h pretreatment with vorinostat can combine with gesicle-mediated delivery of dCas9-VPR to enhance proviral

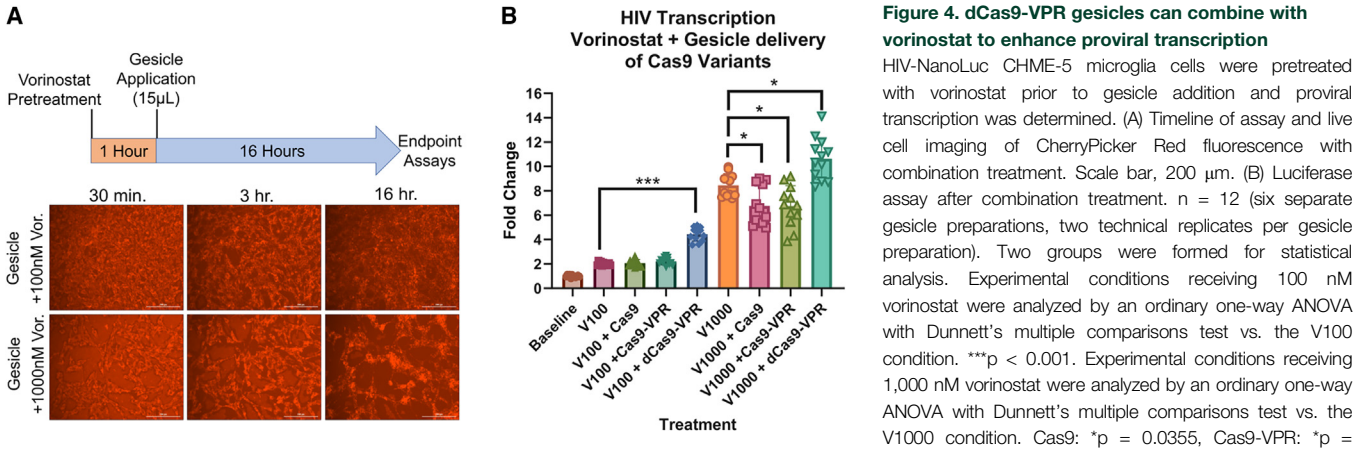

Figure 4. dCas9-VPR gesicles can combine with vorinostat to enhance proviral transcription

HIV-NanoLuc CHME-5 microglia cells were pretreated with vorinostat prior to gesicle addition and proviral transcription was determined. (A) Timeline of assay and live cell imaging of CherryPicker Red fluorescence with combination treatment. Scale bar, 200 μm. (B) Luciferase assay after combination treatment. n = 12 (six separate gesicle preparations, two technical replicates per gesicle preparation). Two groups were formed for statistical analysis. Experimental conditions receiving 100 nM vorinostat were analyzed by an ordinary one-way ANOVA with Dunnett's multiple comparisons test vs. the V100 condition. ***$p < 0.001$. Experimental conditions receiving 1,000 nM vorinostat were analyzed by an ordinary one-way ANOVA with Dunnett's multiple comparisons test vs. the V1000 condition. Cas9: *$p = 0.0355$, Cas9-VPR: *$p = 0.0391$, dCas9-VPR *$p = 0.0148$. Data are expressed as the mean (SD).

transcription. This differs with the previously discussed study where stable transduction and expression of CRISPR activators occurred first, before vorinostat was added to enhance latency reversal.[62]

It is important to note that various cells and tissues throughout the body can harbor latent HIV, such as myeloid-derived cells and certain T cell populations (e.g., CD4+, Central Memory).[12] Additionally, various HIV-infected cell lines differ from each other in the mechanisms that govern latent HIV infection.[65] Moving forward, it would be beneficial to examine the latency reversal effects of vorinostat coupled with gesicle-mediated delivery of dCas9-VPR in additional HIV-infected cell lines before translating the approach to primary cells and *in vivo* models of HIV latency. Indeed, there can be clear differences in the efficacy and outcomes of latency reversal depending on cell type. For instance, vorinostat treatment caused proviral transcription/latency reversal in both HIV-NanoLuc CHME-5 microglia and J-Lat 10.6 lymphocytes but caused decreased proliferation in microglia that contrasted the loss of viability in lymphocytes. Additionally, while dCas9-VPR gesicles successfully combined with vorinostat in HIV-NanoLuc CHME-5, there was less of a clear effect with J-Lat 10.6. Thus, further experiments exploring the effects in different cell types should be conducted in future experiments. Furthermore, additional experiments investigating the effect of gRNA placement throughout the LTR, as well as experiments combining dCas9-VPR gesicles with other LRA classes (e.g., TLR or PKA activators) would be warranted.

In terms of future translation to a clinical setting, several aspects should be addressed. First, a procedure to mass produce and purify gesicles would be needed for potential *in vivo*/*ex vivo* experimentation. Gesicles are essentially non-viral, VSV-G pseudotyped microvesicles. One approach would be to translate techniques including liquid chromatography and suspension culture that are used to produce and purify lentiviral vectors.[66,67] Furthermore, while VSV-G has a wide tropism for transducing cells,[68–70] it would be interesting to know if gesicles can be produced through the overexpression of other viral envelops including those from feline endogenous retroviruses, measles, cocal virus, and others.[71] For clinical utilization, the main benefit of the gesicle system is the delivery of Cas9 variants in ribonucleoprotein (RNP) form. We and others[72,73] have noted that this form of delivery rapidly transfers an already bioactive Cas9 to the recipient cell, which is then degraded within 24 h. This may decrease the time needed to observe a therapeutic effect when compared with lentiviral or adeno-associated virus modalities, which still require viral infection, followed by transcription and translation of the CRISPR-Cas9 components. Moreover, the relatively fast degradation of Cas9 suggests that this method is amenable to more rigorous/frequent dosing strategies. This is key in treatment regimens that will utilize multiple therapeutics, such as the gesicle and vorinostat combination strategy proposed within our data. Furthermore, a newer paper suggests that lipid nanoparticles were superior at mediating delivery and viability in chimeric antigen receptor T cell engineering.[74] Perhaps the gesicle system can be utilized to quickly modify cells *ex vivo* before reintroduction for their *in vivo* therapeutic effect. An example of this in terms of HIV would be CCR5 mutation/deletion in T cells.[75–77] Nevertheless, the direct next steps would include discovering the *in vivo* bioavailability/distribution of gesicles when delivered systemically, and to directly compare gesicle vs. viral (lentivirus, adeno-associated virus) therapeutic intervention in models of replication competent HIV infection. Overall, the current data lay a foundation for these future studies and support the idea that gesicle-mediated delivery of dCas9-VPR may be a useful alternative approach to promote HIV proviral transcription alone, or in combination with other latency-reversing agents.

MATERIALS AND METHODS

Cell culture and treatments

HEK293FT or HIV-NanoLuc CHME-5 microglia were grown in growth media: high-glucose DMEM (GIBCO/Thermo Fisher, Waltham, MA) supplemented with 10% FBS (GIBCO) and 1% antibiotic/antimycotic (GIBCO) and incubated at 5% CO_2, 37°C. Cells were passaged every 4 days using 0.25% trypsin (GIBCO). J-Lat 10.6 lymphocytes were a gift from Dr. Marta Catalfamo. These cells were grown in RPMI 1640 (GIBCO) supplemented with 10% FBS and 1% antibiotic/antimycotic (GIBCO) and were passaged once a week.

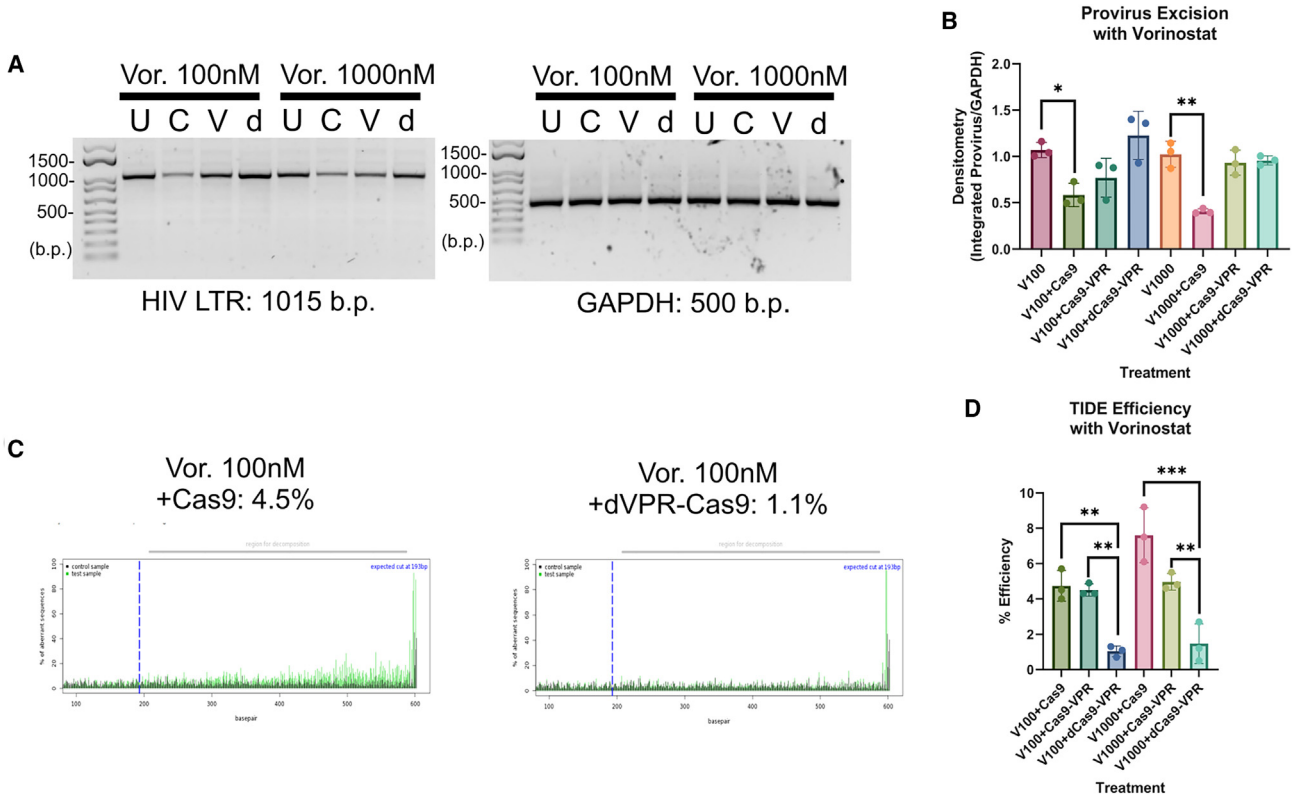

Figure 5. Combining dCas9-VPR with vorinostat does not cause proviral mutation or excision

Molecular assays were performed on HIV-NanoLuc CHME-5 microglia after combination treatment. (A) Representative data of excision assay. Gel electrophoresis for the HIV LTR and GAPDH (U: untreated, C: Cas9, V: Cas9-VPR, d: dCas9-VPR). (B) Densitometric analysis of excision after combination treatment. n = 3 (three separate gesicle preparations). Two groups were formed for statistical analysis. Experimental conditions receiving 100 nM vorinostat were analyzed by an ordinary one-way ANOVA with Dunnett's multiple comparisons test vs. the V100 condition. *p = 0.0173. Experimental conditions receiving 1000 nM vorinostat were analyzed by an ordinary one-way ANOVA with Dunnett's multiple comparisons test vs. the V1000 condition. **p = 0.022. (C) Representative data of TIDE analysis. TIDE aberrant signal sequence graph. A rise in green bars denotes differences in untreated vs. experimental sample. (D) Efficiency score after combination treatment. n = 3 (three separate gesicle preparations). Statistical analysis for TIDE experiments were performed by an ordinary one-way ANOVA with Tukey's multiple comparisons test. **p = 0.0031 V100+Cas9 vs. V100+dCas9-VPR, **p = 0.0052 V100+Cas9-VPR vs. V100+dCas9-VPR; ***p < 0.001 V1000+Cas9 vs. V1000+dCas9 VPR, **p = 0.0048 V1000+Cas9-VPR vs. V1000+dCas9-VPR. Data are expressed as the mean (SD).

Gesicle production

Gesicles were prepared over a 6-day period by standard calcium chloride transfection of HEK293FT cells. Day 1: HEK293FT cells were plated at 4.5×10^6 cells on a 10-cm dish in 10 mL of growth media. Day 2: Two tubes were prepared for transfection. Tube 1 contained 62 µL of 2M $CaCl_2$, the following amounts of DNA (VSV-G 10 µg, CherryPicker Red 2 µg, Cas9 variants 7 µg, gRNA 3 µg), and molecular-grade water to a total volume of 500 µL. Regarding the Cas9 variants, Cas9 (spCas9) was acquired from the Takara/Clontech Gesicle Kit (Takara Bio USA, San Jose, CA), Cas9-VPR (Addgene #68497) and dCas9-VPR (Addgene #63798) were acquired from Addgene (Watertown, MA, plasmids donated by Dr. George Church). The gRNA sequence (LTR gRNA 5′-TTCTACAAGGGACTTTCCGC-3′) was developed to target the HIV-1 (pYU2 GenBank: M93258.1) LTR region using crispor.tefor.net and has been previously used to mutate and excise integrated HIV proviruses.[41] J-Lat 10.6 guide RNA sequence (5′-TGCTACAAGGGACTTTCCGC-3′) was derived from the sequenced genome[45] and targets the exact region as the HIV-NanoLuc CHME-5 gRNA, with 1-bp difference (2nd nucleotide). Tube 2 contained 500 µL of 2xHBS (Sigma-Aldrich, St. Louis, MO). Tube 1 was added to Tube 2 dropwise under gentle agitation, incubated for 20 min, and the entire 1-mL volume was added dropwise to HEK293FT cells. Day 3: A complete media exchange was performed with 15 mL of fresh growth media. Gesicles were allowed to produce gesicles until Day 5. Day 5: the media was collected, centrifuged at 1,500 RPM for 10 min to remove cells and large debris, supernant was filtered through a 0.45-mm syringe, and finally spun at 8,000 relative centrifugal force (RCF), 4°C for 16 h in an ultracentrifuge (Beckman-Coulter, Brea, CA, USA). Day 6: The supernant was discarded and pellet was resuspended in 60 µL PBS and aliquoted for use. Using the current isolation methods, all gesicle preparations contained a heterogeneous mix of exosomes, microvesicles, and apoptotic bodies.

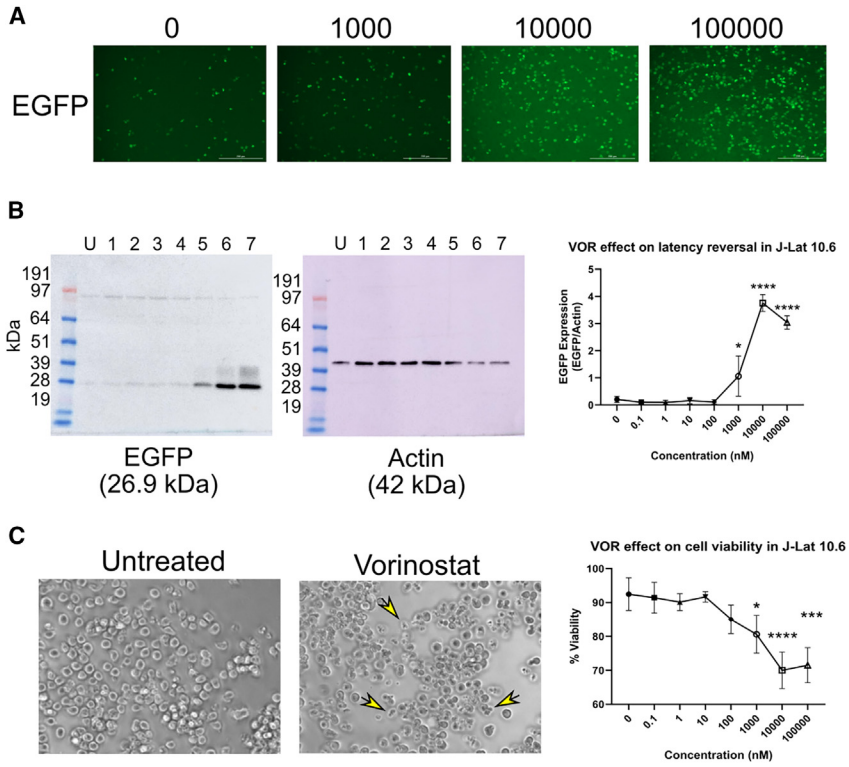

Figure 6. Vorinostat causes latency reversal and decreased viability in J-Lat 10.6 lymphocytes

J-Lat 10.6 lymphocytes were treated with vorinostat at increasing concentrations to create a dose-response relationship. (A) Representative live cell images of EGFP fluorescence in untreated cells (0) or cells treated with vorinostat (1,000, 10,000, 100,000 nM). (B) Western blot analysis of EGFP (26.9 kDa) or actin (42 kDa) and densitometric quantification. U = untreated cells, 1–7 = 10-fold increase in vorinostat concentration starting from 0.1 nM to 100000 nM n = 3 (3 cell passages). Statistical analysis was performed by an ordinary one-way ANOVA with Dunnett's multiple comparisons test vs. the untreated (U/0) control. *p = 0.0183, ****p < 0.0001. (C) Representative phase-contrast images of J-Lat 10.6 cells with or without vorinostat treatment (1000 nM, yellow arrows denote aberrant cell morphology), and trypan blue viability assay. n = 3 (cell passages) Statistical analysis was performed by an ordinary one-way ANOVA with Dunnett's multiple comparisons test vs. the untreated (U/0) control. *p = 0.025, ***p < 0.001, ****p < 0.0001. Data are expressed as the mea - (SD).

Western blot

Cell lysates for western blot analysis were produced using radioimmunoprecipitation assay (RIPA) buffer (Thermo Fisher, Waltham, MA) supplemented with 1% Protease-Phosphotase inhibitor (Thermo Fisher, Waltham, MA). Cells were lysed for 20 min on a rotating plate at 4°C, after which lysates were collected and spun down for 10 min at 10,000 revolutions/min (RPM; 9,400 RCF) in a microcentrifuge. The supernatant was extracted, and protein levels were read using the Pierce BCA Protein Assay Kit (Thermo Fisher, Waltham, MA). Protein lysate was normalized to 30 mg per treatment, and concentrated gesicles were loaded at a 15 μL volume. Samples were separated on a NuPage 4%–12% Bis-Tris gel (Thermo Fisher, Waltham, MA). Protein was transferred to a Novex 0.45-mm polyvinylidene fluoride (PVDF) membrane (Thermo Fisher, Waltham, MA), washed with PBS, and blocked with 5% Immunoanalytical Grade Blotto (Rockland Immunochemicals, Limerick, PA, USA) for 1 h at 24°C. Primary antibodies were diluted in 5% Blotto at a 1:1,000 dilution and incubated overnight at 4°C on a rotating shaker. Primary antibodies used were as follows: VSV-G (Cat. no. v4888; Sigma-Aldrich), Cas9 (Cat. no. MAC133; Millipore, Burlington, MA, USA), EGFP (Cat. no. 50430-2-AP; Proteintech, Rosemont, IL), β-actin (Cat. no. ab3280; Abcam, Cambridge, UK). After primary antibody addition, membranes were washed with PBS three times, and secondary antibody was applied in 5% Blotto for 1 h. Secondary antibodies used were anti-Rabbit HRP (Cat. no. ab205718, Abcam, Cambridge, UK) and anti-Mouse HRP (Cat. no. ab97023, Abcam, Cambridge, UK). After secondary addition, membranes were washed three times with PBS and incubated for 1 min with Pierce ECL Western Blotting Substrate (Thermo Fisher, Waltham, MA). Images were acquired using a GE Scanner (General Electric, Boston, MA).

Gesicle application

HIV-NanoLuc CHME-5 microglia were plated on a Nuclon Delta-treated 96-well plates (either clear or opaque white, Thermo Fisher, Waltham, MA) at 25,000 cells per well in 200 μL of growth media. On the day of gesicle application, media were changed to growth media supplemented with protamine sulfate (8 mg/mL). Gesicles were added (15 μL per well) and centrifuged at 1,150 RCF for 30 min. Cells were returned to the incubator until endpoint assays were conducted. J-Lat 10.6 was plated on a Nuclon Delta-treated 96-well clear plate at 25,000 cells per well in 200 μL of growth media. Due to the cell type being a suspension culture, 30 μL of gesicles were used per well and the remaining procedure was carried out as described.

Luciferase assay

The luciferase assay was performed 16 h post gesicle treatment. Media from the 96-well plates were aspirated and washed with 1xPBS before RIPA buffer (75 μL) was added onto cell lysis as previously described. Coelenterazine (Regis Technologies, Morton Grove, IL) was added to the cells (10 μM final concentration, 100 μL per well) before luminescence was assayed on a Spectramax Id3 plate reader (Molecular Devices, San Jose, CA).

PCR/excision assay

Cells used for molecular characterization were treated with gesicles and/or vorinostat for 16 h, after which media was aspirated, and cells were washed with 1xPBS before fresh media was added. Cells were expanded from a 96-well plate to a 12-well plate over the course of

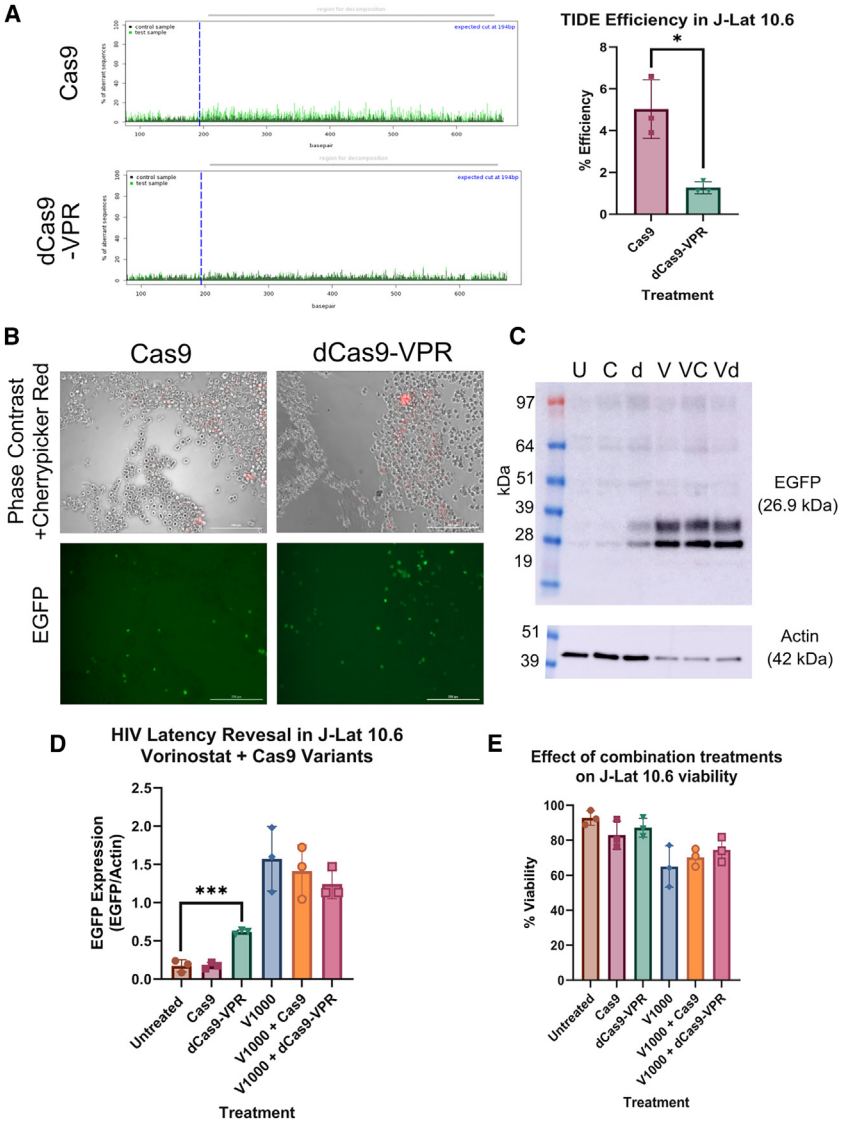

Figure 7. dCas9-VPR gesicles can reverse latency in J-Lat 10.6 lymphocytes

dCas9-VPR gesicles were applied to J-Lat 10.6 lymphocytes alone or in combination with vorinostat to determine latency reversal. (A) A TIDE analysis was performed using Cas9 and dCas9-VPR due to a single nucleotide difference between gRNA sequences of HIV-NanoLuc CHME-5 and J-Lat 10.6 n = 3 (3 separate gesicle preparations). Statistical analysis was performed by an unpaired t test. *p = 0.0103. (B) Live cell images localizing gesicle expression (CherryPicker Red) and cell morphology. EGFP expression denotes latency reversal. (C) Western Blot analysis of Cas9 and dCas9 gesicles alone or in combination with 1,000 nM vorinostat. U = untreated, C = Cas9, d = dCas9-VPR, V = vorinostat, VC = vorinostat + Cas9, Vd = vorinostat + dCas9-VPR. (D) Densitometric analysis. n = 3 (3 separate gesicle preparations). Two groups were formed for statistical analysis. Experimental conditions not receiving vorinostat were analyzed by an ordinary one-way ANOVA with Dunnett's multiple comparisons test vs. the Untreated condition. ***p < 0.001. Experimental conditions receiving 1000 nM vorinostat were analyzed by an ordinary one-way ANOVA with Dunnett's multiple comparisons test vs. the V1000 condition. (E) Trypan blue viability assay. n = 3 (three separate gesicle preparations). No significant effects on viability within groups.

5 days. This procedure was performed to obtain adequate DNA yields for the subsequent experiments, as previous experiments trying to obtain genomic DNA from a 96-well format result in undetectable levels with some samples. The genomic DNA was isolated using the NucleoSpin Tissue Column (Macherey-Nagel, Bethlehem, PA, USA) according to the manufacturer's instructions. DNA concentrations were approximated by A260 reading, using a NanoDrop 2000 (Thermo Fisher, Waltham, MA). PCRs were prepared using Taq 2x Mastermix (New England Biolabs, Ipswich, MA, USA) with 5 μM forward and reverse primers and 100 ng of DNA sample. PCR was carried out in an Eppendorf Thermal Cycler (Eppendorf, Enfield, CA) using the following cycle: 95°C for 30 s, 30x cycles of 95°C for 22 s → 55°C for 45 s → 68°C for 5 min, 68°C for 5 min, and a 4°C hold. PCR products were run on a 1% agarose gel made with 1x TAE (Invitrogen, Waltham, MA) with SYBR Safe DNA gel stain (Thermo Fisher, Waltham, MA) for 50 min at 150 V. The excision assay was analyzed by determining band densitometry of LTR amplification divided by GAPDH using FIJI/ImageJ. List of primer sets used are below.

TIDE analysis

Resulting bands from the LTR PCR amplification were excised and gel purified using the Nucleospin Gel and PCR Clean Up kit (Macherey-Nagel, Bethlehem, PA, USA) and DNA concentrations were analyzed by a NanoDrop 2000 (Thermo Fisher, Waltham, MA). Purified PCR product was sent for Sanger sequencing (Genewiz-Azenta, Burlington, MA) and sequences were uploaded to TIDE for analysis of indels.

Drug treatments/cell viability and proliferation

Drugs were purchased from Sigma (Sigma-Aldrich, St. Louis, MO): Lipopolysaccharide (L2630-10MG), resiquimod (SML0196-10MG), and vorinostat (SML0061-5MG) and prepared as per the manufacturer's instructions. Drugs were diluted in growth media at the listed concentrations (0.1 nM–100,000 nM) and added to HIV-NanoLuc CHME-5 microglia by a full media exchange. After treatment (16 h) a luciferase assay was performed. Viability assays were performed using a Promega Cell-Titer Glow Luminescent Viability Assay (Promega, Madison, WI). Hoechst staining (Thermo Fisher, Waltham, MA), was performed after vorinostat treatment and cells were counted using the Lionheart Imager and Gen5 software (Agilent, Santa Clara, CA). Because J-Lat 10.6 lymphocytes are a suspension

culture, viability was assayed by trypan blue staining and cell counting using the Countess 3 Automated Cell Counter (Thermo Fisher, Waltham, MA) according to the manufacturer's instructions.

Gesicle and vorinostat combination experiments

In experiments combining gesicles with vorinostat, vorinostat was applied to cells as a 1-h pretreatment step. Gesicles (15 μL for HIV-NanoLuc CHME-5 or 30 μL for J-Lat 10.6) were then spiked into the media and centrifuged as previously described. Therefore, cells were exposed to both vorinostat and gesicles for the reminder of the treatment time course.

Live cell imaging

HIV-NanoLuc CHME-5 microglia were live cell imaged using a Lionheart Imager and Gen5 software (Agilent, Santa Clara, CA). In brief, the microscope incubator was set to 5% CO_2, 37°C, and humidified. Brightfield and/or Texas Red channels were imaged every 15 min for a total of 16 h.

Statistical analysis and data processing

Data processing was only performed for luciferase assays measuring HIV proviral transcription. Raw luminescence values were normalized to the baseline luminescence of untreated cells to create fold-change graphs. All data were analyzed using GraphPad Prism 9 (GraphPad, San Diego, CA). Statistical analysis was performed where appropriate by three different tests including an ordinary one-way ANOVA with Dunnett's multiple comparisons test, an ordinary one-way ANOVA with Tukey's multiple comparisons test, and an unpaired t test.

DATA AND CODE AVAILABILITY

The data that support the findings of this study are available from the corresponding author, Campbell, LA, upon reasonable request.

ACKNOWLEDGMENTS

This work was not supported by a specific granting mechanism.

AUTHOR CONTRIBUTIONS

M.A.F. performed experiments (western blots, all dose-response/viability experiments, PCR primer design, gesicle treatment, molecular analysis, etc.) and wrote the manuscript (abstract, graphical abstract, introduction, discussion). W.C. performed experiments (J-Lat 10.6 dose-response curves, imaging, western blot analysis). L.A.C. designed experiments (overarching goals, endpoint analysis), performed experiments (gesicles preparation, gesicle treatment, molecular analysis etc.), and wrote the manuscript (materials and methods, results, figures and figure legends, editing).

DECLARATION OF INTERESTS

The authors declare no competing interests.

REFERENCES

1. UNAIDS. UNAIDS Fact Sheet- Latest Global and Regional Statistics on the Status of the AIDS Epidemic. 2023.
2. Vidya Vijayan, K.K., Karthigeyan, K.P., Tripathi, S.P., and Hanna, L.E. (2017). Pathophysiology of CD4+ T-Cell Depletion in HIV-1 and HIV-2 Infections. Front. Immunol. *8*, 580. https://doi.org/10.3389/fimmu.2017.00580.
3. Deeks, S.G., Overbaugh, J., Phillips, A., and Buchbinder, S. (2015). HIV infection. Nat. Rev. Dis. Primers *1*, 15035. https://doi.org/10.1038/nrdp.2015.35.
4. Castro-Gonzalez, S., Colomer-Lluch, M., and Serra-Moreno, R. (2018). Barriers for HIV Cure: The Latent Reservoir. AIDS Res. Hum. Retroviruses *34*, 739–759. https://doi.org/10.1089/AID.2018.0118.
5. Jean, M.J., Fiches, G., Hayashi, T., and Zhu, J. (2019). Current Strategies for Elimination of HIV-1 Latent Reservoirs Using Chemical Compounds Targeting Host and Viral Factors. AIDS Res. Hum. Retroviruses *35*, 1–24. https://doi.org/10.1089/AID.2018.0153.
6. Eisele, E., and Siliciano, R.F. (2012). Redefining the viral reservoirs that prevent HIV-1 eradication. Immunity *37*, 377–388. https://doi.org/10.1016/j.immuni.2012.08.010.
7. Richman, D.D., Margolis, D.M., Delaney, M., Greene, W.C., Hazuda, D., and Pomerantz, R.J. (2009). The challenge of finding a cure for HIV infection. Science *323*, 1304–1307. https://doi.org/10.1126/science.1165706.
8. Pasternak, A.O., and Berkhout, B. (2023). HIV persistence: silence or resistance? Curr. Opin. Virol. *59*, 101301. https://doi.org/10.1016/j.coviro.2023.101301.
9. Bandera, A., Gori, A., Clerici, M., and Sironi, M. (2019). Phylogenies in ART: HIV reservoirs, HIV latency and drug resistance. Curr. Opin. Pharmacol. *48*, 24–32. https://doi.org/10.1016/j.coph.2019.03.003.
10. Mata, R.C., Viciana, P., de Alarcón, A., López-Cortés, L.F., Gómez-Vera, J., Trastoy, M., and Cisneros, J.M. (2005). Discontinuation of antiretroviral therapy in patients with chronic HIV infection: clinical, virologic, and immunologic consequences. AIDS Patient Care STDS *19*, 550–562. https://doi.org/10.1089/apc.2005.19.550.
11. García, F., Plana, M., Vidal, C., Cruceta, A., O'Brien, W.A., Pantaleo, G., Pumarola, T., Gallart, T., Miró, J.M., and Gatell, J.M. (1999). Dynamics of viral load rebound and immunological changes after stopping effective antiretroviral therapy. AIDS *13*, F79–F86. https://doi.org/10.1097/00002030-199907300-00002.
12. Chen, J., Zhou, T., Zhang, Y., Luo, S., Chen, H., Chen, D., Li, C., and Li, W. (2022). The reservoir of latent HIV. Front. Cell. Infect. Microbiol. *12*, 945956. https://doi.org/10.3389/fcimb.2022.945956.
13. Finzi, D., Blankson, J., Siliciano, J.D., Margolick, J.B., Chadwick, K., Pierson, T., Smith, K., Lisziewicz, J., Lori, F., Flexner, C., et al. (1999). Latent infection of CD4+ T cells provides a mechanism for lifelong persistence of HIV-1, even in patients on effective combination therapy. Nat. Med. *5*, 512–517. https://doi.org/10.1038/8394.
14. Kumar, A., Abbas, W., and Herbein, G. (2014). HIV-1 latency in monocytes/macrophages. Viruses *6*, 1837–1860. https://doi.org/10.3390/v6041837.
15. Keele, B.F., Tazi, L., Gartner, S., Liu, Y., Burgon, T.B., Estes, J.D., Thacker, T.C., Crandall, K.A., McArthur, J.C., and Burton, G.F. (2008). Characterization of the follicular dendritic cell reservoir of human immunodeficiency virus type 1. J. Virol. *82*, 5548–5561. https://doi.org/10.1128/JVI.00124-08.
16. Carter, C.C., Onafuwa-Nuga, A., McNamara, L.A., Riddell, J., Bixby, D., Savona, M.R., and Collins, K.L. (2010). HIV-1 infects multipotent progenitor cells causing cell death and establishing latent cellular reservoirs. Nat. Med. *16*, 446–451. https://doi.org/10.1038/nm.2109.
17. Churchill, M.J., Gorry, P.R., Cowley, D., Lal, L., Sonza, S., Purcell, D.F.J., Thompson, K.A., Gabuzda, D., McArthur, J.C., Pardo, C.A., and Wesselingh, S.L. (2006). Use of laser capture microdissection to detect integrated HIV-1 DNA in macrophages and astrocytes from autopsy brain tissues. J. Neurovirol. *12*, 146–152. https://doi.org/10.1080/13550280600748946.
18. Wallet, C., De Rovere, M., Van Assche, J., Daouad, F., De Wit, S., Gautier, V., Mallon, P.W.G., Marcello, A., Van Lint, C., Rohr, O., and Schwartz, C. (2019). Microglial Cells: The Main HIV-1 Reservoir in the Brain. Front. Cell. Infect. Microbiol. *9*, 362. https://doi.org/10.3389/fcimb.2019.00362.
19. Archin, N.M., Kirchherr, J.L., Sung, J.A., Clutton, G., Sholtis, K., Xu, Y., Allard, B., Stuelke, E., Kashuba, A.D., Kuruc, J.D., et al. (2017). Interval dosing with the HDAC inhibitor vorinostat effectively reverses HIV latency. J. Clin. Invest. *127*, 3126–3135. https://doi.org/10.1172/JCI92684.

20. Kula-Pacurar, A., Rodari, A., Darcis, G., and Van Lint, C. (2021). Shocking HIV-1 with immunomodulatory latency reversing agents. Semin. Immunol. *51*, 101478. https://doi.org/10.1016/j.smim.2021.101478.

21. Archin, N.M., Liberty, A.L., Kashuba, A.D., Choudhary, S.K., Kuruc, J.D., Crooks, A.M., Parker, D.C., Anderson, E.M., Kearney, M.F., Strain, M.C., et al. (2012). Administration of vorinostat disrupts HIV-1 latency in patients on antiretroviral therapy. Nature *487*, 482–485. https://doi.org/10.1038/nature11286.

22. Archin, N.M., Keedy, K.S., Espeseth, A., Dang, H., Hazuda, D.J., and Margolis, D.M. (2009). Expression of latent human immunodeficiency type 1 is induced by novel and selective histone deacetylase inhibitors. AIDS *23*, 1799–1806. https://doi.org/10.1097/QAD.0b013e32832ec1dc.

23. Contreras, X., Schweneker, M., Chen, C.S., McCune, J.M., Deeks, S.G., Martin, J., and Peterlin, B.M. (2009). Suberoylanilide hydroxamic acid reactivates HIV from latently infected cells. J. Biol. Chem. *284*, 6782–6789. https://doi.org/10.1074/jbc.M807898200.

24. Elliott, J.H., Wightman, F., Solomon, A., Ghneim, K., Ahlers, J., Cameron, M.J., Smith, M.Z., Spelman, T., McMahon, J., Velayudham, P., et al. (2014). Activation of HIV transcription with short-course vorinostat in HIV-infected patients on suppressive antiretroviral therapy. PLoS Pathog. *10*, e1004473. https://doi.org/10.1371/journal.ppat.1004473.

25. Ma, Y., Zhang, L., and Huang, X. (2014). Genome modification by CRISPR/Cas9. FEBS J. *281*, 5186–5193. https://doi.org/10.1111/febs.13110.

26. Magro, G., Calistri, A., and Parolin, C. (2021). Targeting and Understanding HIV Latency: The CRISPR System against the Provirus. Pathogens *10*, 1257. https://doi.org/10.3390/pathogens10101257.

27. Darcis, G., Das, A.T., and Berkhout, B. (2018). Tackling HIV Persistence: Pharmacological versus CRISPR-Based Shock Strategies. Viruses *10*, 157. https://doi.org/10.3390/v10040157.

28. Xu, Y., Peng, X., Zheng, Y., Jin, C., Lu, X., Han, D., Fu, H., Chen, C., and Wu, N. (2021). Inactivation of Latent HIV-1 Proviral DNA Using Clustered Regularly Interspaced Short Palindromic Repeats/Cas9 Treatment and the Assessment of Off-Target Effects. Front. Microbiol. *12*, 629153. https://doi.org/10.3389/fmicb.2021.629153.

29. Zhang, Y., Yin, C., Zhang, T., Li, F., Yang, W., Kaminski, R., Fagan, P.R., Putatunda, R., Young, W.B., Khalili, K., and Hu, W. (2015). CRISPR/gRNA-directed synergistic activation mediator (SAM) induces specific, persistent and robust reactivation of the HIV-1 latent reservoirs. Sci. Rep. *5*, 16277. https://doi.org/10.1038/srep16277.

30. Bialek, J.K., Dunay, G.A., Voges, M., Schäfer, C., Spohn, M., Stucka, R., Hauber, J., and Lange, U.C. (2016). Targeted HIV-1 Latency Reversal Using CRISPR/Cas9-Derived Transcriptional Activator Systems. PLoS One *11*, e0158294. https://doi.org/10.1371/journal.pone.0158294.

31. Konermann, S., Brigham, M.D., Trevino, A.E., Joung, J., Abudayyeh, O.O., Barcena, C., Hsu, P.D., Habib, N., Gootenberg, J.S., Nishimasu, H., et al. (2015). Genome-scale transcriptional activation by an engineered CRISPR-Cas9 complex. Nature *517*, 583–588. https://doi.org/10.1038/nature14136.

32. Tanenbaum, M.E., Gilbert, L.A., Qi, L.S., Weissman, J.S., and Vale, R.D. (2014). A protein-tagging system for signal amplification in gene expression and fluorescence imaging. Cell *159*, 635–646. https://doi.org/10.1016/j.cell.2014.09.039.

33. Saayman, S.M., Lazar, D.C., Scott, T.A., Hart, J.R., Takahashi, M., Burnett, J.C., Planelles, V., Morris, K.V., and Weinberg, M.S. (2016). Potent and Targeted Activation of Latent HIV-1 Using the CRISPR/dCas9 Activator Complex. Mol. Ther. *24*, 488–498. https://doi.org/10.1038/mt.2015.202.

34. Sadowski, I., Ma, J., Triezenberg, S., and Ptashne, M. (1988). GAL4-VP16 is an unusually potent transcriptional activator. Nature *335*, 563–564. https://doi.org/10.1038/335563a0.

35. Chavez, A., Scheiman, J., Vora, S., Pruitt, B.W., Tuttle, M., P R Iyer, E., Lin, S., Kiani, S., Guzman, C.D., Wiegand, D.J., et al. (2015). Highly efficient Cas9-mediated transcriptional programming. Nat. Methods *12*, 326–328. https://doi.org/10.1038/nmeth.3312.

36. Klinnert, S., Chemnitzer, A., Rusert, P., and Metzner, K.J. (2022). Systematic HIV-1 promoter targeting with CRISPR/dCas9-VPR reveals optimal region for activation of the latent provirus. J. Gen. Virol. *103*, 1–13. https://doi.org/10.1099/jgv.0.001754.

37. Mangeot, P.E., Dollet, S., Girard, M., Ciancia, C., Joly, S., Peschanski, M., and Lotteau, V. (2011). Protein transfer into human cells by VSV-G-induced nanovesicles. Mol. Ther. *19*, 1656–1666. https://doi.org/10.1038/mt.2011.138.

38. Campbell, L.A., Richie, C.T., Maggirwar, N.S., and Harvey, B.K. (2019). Cas9 Ribonucleoprotein Complex Delivery: Methods and Applications for Neuroinflammation. J. Neuroimmune Pharmacol. *14*, 565–577. https://doi.org/10.1007/s11481-019-09856-z.

39. Anders, C., and Jinek, M. (2014). In vitro enzymology of Cas9. Methods Enzymol. *546*, 1–20. https://doi.org/10.1016/B978-0-12-801185-0.00001-5.

40. Karlson, C.K.S., Mohd-Noor, S.N., Nolte, N., and Tan, B.C. (2021). CRISPR/dCas9-Based Systems: Mechanisms and Applications in Plant Sciences. Plants *10*, 2055. https://doi.org/10.3390/plants10102055.

41. Campbell, L.A., Richie, C.T., Zhang, Y., Heathward, E.J., Coke, L.M., Park, E.Y., and Harvey, B.K. (2017). In vitro modeling of HIV proviral activity in microglia. FEBS J. *284*, 4096–4114. https://doi.org/10.1111/febs.14293.

42. Brinkman, E.K., Chen, T., Amendola, M., and van Steensel, B. (2014). Easy quantitative assessment of genome editing by sequence trace decomposition. Nucleic Acids Res. *42*, e168. https://doi.org/10.1093/nar/gku936.

43. Park, S.Y., and Kim, J.S. (2020). A short guide to histone deacetylases including recent progress on class II enzymes. Exp. Mol. Med. *52*, 204–212. https://doi.org/10.1038/s12276-020-0382-4.

44. Heinbockel, L., Weindl, G., Martinez-de-Tejada, G., Correa, W., Sanchez-Gomez, S., Bárcena-Varela, S., Goldmann, T., Garidel, P., Gutsmann, T., and Brandenburg, K. (2018). Inhibition of Lipopolysaccharide- and Lipoprotein-Induced Inflammation by Antitoxin Peptide Pep19-2.5. Front. Immunol. *9*, 1704. https://doi.org/10.3389/fimmu.2018.01704.

45. Chung, C.H., Mele, A.R., Allen, A.G., Costello, R., Dampier, W., Nonnemacher, M.R., and Wigdahl, B. (2020). Integrated Human Immunodeficiency Virus Type 1 Sequence in J-Lat 10.6. Microbiol. Resour. Announc. *9*, e00179-20. https://doi.org/10.1128/MRA.00179-20.

46. Jordan, A., Bisgrove, D., and Verdin, E. (2003). HIV reproducibly establishes a latent infection after acute infection of T cells in vitro. EMBO J. *22*, 1868–1877. https://doi.org/10.1093/emboj/cdg188.

47. Sarfstein, R., Bruchim, I., Fishman, A., and Werner, H. (2011). The mechanism of action of the histone deacetylase inhibitor vorinostat involves interaction with the insulin-like growth factor signaling pathway. PLoS One *6*, e24468. https://doi.org/10.1371/journal.pone.0024468.

48. Bernhart, E., Stuendl, N., Kaltenegger, H., Windpassinger, C., Donohue, N., Leithner, A., and Lohberger, B. (2017). Histone deacetylase inhibitors vorinostat and panobinostat induce G1 cell cycle arrest and apoptosis in multidrug resistant sarcoma cell lines. Oncotarget *8*, 77254–77267. https://doi.org/10.18632/oncotarget.20460.

49. Kurundkar, D., Srivastava, R.K., Chaudhary, S.C., Ballestas, M.E., Kopelovich, L., Elmets, C.A., and Athar, M. (2013). Vorinostat, an HDAC inhibitor attenuates epidermoid squamous cell carcinoma growth by dampening mTOR signaling pathway in a human xenograft murine model. Toxicol. Appl. Pharmacol. *266*, 233–244. https://doi.org/10.1016/j.taap.2012.11.002.

50. Bubna, A.K. (2015). Vorinostat-An Overview. Indian J. Dermatol. *60*, 419. https://doi.org/10.4103/0019-5154.160511.

51. Ho, Y.C., Shan, L., Hosmane, N.N., Wang, J., Laskey, S.B., Rosenbloom, D.I.S., Lai, J., Blankson, J.N., Siliciano, J.D., and Siliciano, R.F. (2013). Replication-competent noninduced proviruses in the latent reservoir increase barrier to HIV-1 cure. Cell *155*, 540–551. https://doi.org/10.1016/j.cell.2013.09.020.

52. Saayman, S., Ali, S.A., Morris, K.V., and Weinberg, M.S. (2015). The therapeutic application of CRISPR/Cas9 technologies for HIV. Expert Opin. Biol. Ther. *15*, 819–830. https://doi.org/10.1517/14712598.2015.1036736.

53. Ji, H., Jiang, Z., Lu, P., Ma, L., Li, C., Pan, H., Fu, Z., Qu, X., Wang, P., Deng, J., et al. (2016). Specific Reactivation of Latent HIV-1 by dCas9-SunTag-VP64-mediated Guide RNA Targeting the HIV-1 Promoter. Mol. Ther. *24*, 508–521. https://doi.org/10.1038/mt.2016.7.

54. Cho, S.W., Kim, S., Kim, Y., Kweon, J., Kim, H.S., Bae, S., and Kim, J.S. (2014). Analysis of off-target effects of CRISPR/Cas-derived RNA-guided endonucleases and nickases. Genome Res. *24*, 132–141. https://doi.org/10.1101/gr.162339.113.

55. Fu, Y., Foden, J.A., Khayter, C., Maeder, M.L., Reyon, D., Joung, J.K., and Sander, J.D. (2013). High-frequency off-target mutagenesis induced by CRISPR-Cas nucleases in human cells. Nat. Biotechnol. *31*, 822–826. https://doi.org/10.1038/nbt.2623.

56. Hsu, P.D., Scott, D.A., Weinstein, J.A., Ran, F.A., Konermann, S., Agarwala, V., Li, Y., Fine, E.J., Wu, X., Shalem, O., et al. (2013). DNA targeting specificity of RNA-guided Cas9 nucleases. Nat. Biotechnol. *31*, 827–832. https://doi.org/10.1038/nbt.2647.

57. Uemura, T., Mori, T., Kurihara, T., Kawase, S., Koike, R., Satoga, M., Cao, X., Li, X., Yanagawa, T., Sakurai, T., et al. (2016). Fluorescent protein tagging of endogenous protein in brain neurons using CRISPR/Cas9-mediated knock-in and in utero electroporation techniques. Sci. Rep. *6*, 35861. https://doi.org/10.1038/srep35861.

58. Wang, M., Zuris, J.A., Meng, F., Rees, H., Sun, S., Deng, P., Han, Y., Gao, X., Pouli, D., Wu, Q., et al. (2016). Efficient delivery of genome-editing proteins using bioreducible lipid nanoparticles. Proc. Natl. Acad. Sci. USA *113*, 2868–2873. https://doi.org/10.1073/pnas.1520244113.

59. Momen-Heravi, F., Balaj, L., Alian, S., Mantel, P.Y., Halleck, A.E., Trachtenberg, A.J., Soria, C.E., Oquin, S., Bonebreak, C.M., Saracoglu, E., et al. (2013). Current methods for the isolation of extracellular vesicles. Biol. Chem. *394*, 1253–1262. https://doi.org/10.1515/hsz-2013-0141.

60. De la Torre-Tarazona, H.E., Jiménez, R., Bueno, P., Camarero, S., Román, L., Fernández-García, J.L., Beltrán, M., Nothias, L.F., Cachet, X., Paolini, J., et al. (2020). 4-Deoxyphorbol inhibits HIV-1 infection in synergism with antiretroviral drugs and reactivates viral reservoirs through PKC/MEK activation synergizing with vorinostat. Biochem. Pharmacol. *177*, 113937. https://doi.org/10.1016/j.bcp.2020.113937.

61. Lim, H., Kim, K.C., Son, J., Shin, Y., Yoon, C.H., Kang, C., and Choi, B.S. (2017). Synergistic reactivation of latent HIV-1 provirus by PKA activator dibutyryl-cAMP in combination with an HDAC inhibitor. Virus Res. *227*, 1–5. https://doi.org/10.1016/j.virusres.2016.09.015.

62. Limsirichai, P., Gaj, T., and Schaffer, D.V. (2016). CRISPR-mediated Activation of Latent HIV-1 Expression. Mol. Ther. *24*, 499–507. https://doi.org/10.1038/mt.2015.213.

63. Moj, D., Britz, H., Burhenne, J., Stewart, C.F., Egerer, G., Haefeli, W.E., and Lehr, T. (2017). A physiologically based pharmacokinetic and pharmacodynamic (PBPK/PD) model of the histone deacetylase (HDAC) inhibitor vorinostat for pediatric and adult patients and its application for dose specification. Cancer Chemother. Pharmacol. *80*, 1013–1026. https://doi.org/10.1007/s00280-017-3447-x.

64. O'Connor, O.A., Heaney, M.L., Schwartz, L., Richardson, S., Willim, R., MacGregor-Cortelli, B., Curly, T., Moskowitz, C., Portlock, C., Horwitz, S., et al. (2006). Clinical experience with intravenous and oral formulations of the novel histone deacetylase inhibitor suberoylanilide hydroxamic acid in patients with advanced hematologic malignancies. J. Clin. Oncol. *24*, 166–173. https://doi.org/10.1200/JCO.2005.01.9679.

65. Telwatte, S., Morón-López, S., Aran, D., Kim, P., Hsieh, C., Joshi, S., Montano, M., Greene, W.C., Butte, A.J., Wong, J.K., and Yukl, S.A. (2019). Heterogeneity in HIV and cellular transcription profiles in cell line models of latent and productive infection: implications for HIV latency. Retrovirology *16*, 32. https://doi.org/10.1186/s12977-019-0494-x.

66. Soldi, M., Sergi Sergi, L., Unali, G., Kerzel, T., Cuccovillo, I., Capasso, P., Annoni, A., Biffi, M., Rancoita, P.M.V., Cantore, A., et al. (2020). Laboratory-Scale Lentiviral Vector Production and Purification for Enhanced. Mol. Ther. Methods Clin. Dev. *19*, 411–425. https://doi.org/10.1016/j.omtm.2020.10.009.

67. Bauler, M., Roberts, J.K., Wu, C.C., Fan, B., Ferrara, F., Yip, B.H., Diao, S., Kim, Y.I., Moore, J., Zhou, S., et al. (2020). Production of Lentiviral Vectors Using Suspension Cells Grown in Serum-free Media. Mol. Ther. Methods Clin. Dev. *17*, 58–68. https://doi.org/10.1016/j.omtm.2019.11.011.

68. Page, K.A., Landau, N.R., and Littman, D.R. (1990). Construction and use of a human immunodeficiency virus vector for analysis of virus infectivity. J. Virol. *64*, 5270–5276. https://doi.org/10.1128/JVI.64.11.5270-5276.1990.

69. Naldini, L., Blömer, U., Gallay, P., Ory, D., Mulligan, R., Gage, F.H., Verma, I.M., and Trono, D. (1996). In vivo gene delivery and stable transduction of nondividing cells by a lentiviral vector. Science *272*, 263–267. https://doi.org/10.1126/science.272.5259.263.

70. Reiser, J., Harmison, G., Kluepfel-Stahl, S., Brady, R.O., Karlsson, S., and Schubert, M. (1996). Transduction of nondividing cells using pseudotyped defective high-titer HIV type 1 particles. Proc. Natl. Acad. Sci. USA *93*, 15266–15271. https://doi.org/10.1073/pnas.93.26.15266.

71. Gutierrez-Guerrero, A., Cosset, F.L., and Verhoeyen, E. (2020). Lentiviral Vector Pseudotypes: Precious Tools to Improve Gene Modification of Hematopoietic Cells for Research and Gene Therapy. Viruses *12*, 1016. https://doi.org/10.3390/v12091016.

72. Kim, S., Kim, D., Cho, S.W., Kim, J., and Kim, J.S. (2014). Highly efficient RNA-guided genome editing in human cells via delivery of purified Cas9 ribonucleoproteins. Genome Res. *24*, 1012–1019. https://doi.org/10.1101/gr.171322.113.

73. Lin, S., Staahl, B.T., Alla, R.K., and Doudna, J.A. (2014). Enhanced homology-directed human genome engineering by controlled timing of CRISPR/Cas9 delivery. Elife *3*, e04766. https://doi.org/10.7554/eLife.04766.

74. Kitte, R., Rabel, M., Geczy, R., Park, S., Fricke, S., Koehl, U., and Tretbar, U.S. (2023). Lipid nanoparticles outperform electroporation in mRNA-based CAR T cell engineering. Mol. Ther. Methods Clin. Dev. *31*, 101139. https://doi.org/10.1016/j.omtm.2023.101139.

75. Hütter, G., Nowak, D., Mossner, M., Ganepola, S., Müssig, A., Allers, K., Schneider, T., Hofmann, J., Kücherer, C., Blau, O., et al. (2009). Long-term control of HIV by CCR5 Delta32/Delta32 stem-cell transplantation. N. Engl. J. Med. *360*, 692–698. https://doi.org/10.1056/NEJMoa0802905.

76. Cradick, T.J., Fine, E.J., Antico, C.J., and Bao, G. (2013). CRISPR/Cas9 systems targeting β-globin and CCR5 genes have substantial off-target activity. Nucleic Acids Res. *41*, 9584–9592. https://doi.org/10.1093/nar/gkt714.

77. Tebas, P., Stein, D., Tang, W.W., Frank, I., Wang, S.Q., Lee, G., Spratt, S.K., Surosky, R.T., Giedlin, M.A., Nichol, G., et al. (2014). Gene editing of CCR5 in autologous CD4 T cells of persons infected with HIV. N. Engl. J. Med. *370*, 901–910. https://doi.org/10.1056/NEJMoa1300662.